

Supplementary Information for

Primary Productivity Below the Seafloor at Deep-Sea Hot Springs

Jesse McNichol*, Hryhoriy Stryhanyuk, Sean P. Sylva, François Thomas, Niculina Musat,

Jeffrey S. Seewald, Stefan M. Sievert*

*To whom correspondence should be addressed. Emails: mcnichol@alum.mit.edu;

ssievert@whoi.edu

This PDF file includes:

SI Material and Methods

SI Text

Figs. S1 to S6

Tables S1 to S2

Other supplementary material for this manuscript includes the following:

Dataset S1 (excel file)

SI Text

Extrapolations to natural environment. *In situ* primary productivity at our study site was estimated using two pieces of information. Firstly, depletions in electron acceptors associated with chemosynthesis (nitrate and oxygen) were used to determine the “fingerprint” of microbial activity in the natural environment (1). Then, given the range of values for CGE, we estimated how much carbon could be fixed by microbes that had consumed these substrates during growth *in situ*. This generated values of carbon fixed per volume of mixed diffuse-flow (low-temperature) vent fluid. These values were normalized per volume end-member fluid to compare with values from (2). Normalization was accomplished by considering the fraction of end-member fluid in *Crab Spa* mixed fluids (1).

Standing stock was constrained by estimating the minimum number of cells needed to account for the observed chemical depletions *in situ* using per-cell chemical consumption rates determined previously (1). This calculation was accomplished as follows. Given observed chemical depletions and fluid flux, we first calculated the number of moles of electron acceptors (oxygen and nitrate) consumed at *Crab Spa* per unit time. Next, we assumed that the fluid flux is unidirectional (i.e. there is no recirculation) and that it passes over biofilm microbial communities in the sub-seafloor biosphere responsible for the consumption of the substrates indicated above. Given that these microbes should have a maximal metabolic rate dictated by the turnover time of enzymes and various other factors, we can use metabolic rate estimates to determine the number of cells minimally responsible for signatures of sub-seafloor metabolic activity (i.e. chemical depletions). Estimates of maximal metabolic rates under *in situ* pressure and temperature conditions have been previously reported (1). For the purposes of this

calculation, we assumed that cells are either obligate denitrifiers or use oxygen as a sole electron acceptor. While sulfur species could be also used as electron acceptors, this process is only exergonic with hydrogen as an electron donor. At our study site, predicted concentrations of hydrogen are low compared to the amount of sulfur available, so we neglected sulfur as a potential electron acceptor for the purposes of this calculation. The output of this calculation is an estimate of the minimal number of cells present in the sub-seafloor biosphere necessary to account for the observed depletions.

In order to convert cell numbers to biomass, we used estimates of cell carbon density per unit cell volume. The conversion factor we used to convert NanoSIMS isotope ratios to per-cell carbon fixation rates was determined for small, pelagic cells (3). Since the ratio between NanoSIMS and bulk isotope uptake rate measurements is similar to previously determined values (4), it suggests this was an appropriate conversion factor for our experimental incubations.

Using values for cell size derived from incubations ($0.8 \mu\text{m}^3$) and the biovolume:cell carbon conversion factor mentioned above (3) yields an estimate of $\sim 300 \text{ fg C per cell}$. This value was then multiplied by the number of cells minimally responsible for chemical depletions to determine an estimate of the total biomass standing stock in the sub-seafloor at our study site of $\sim 1 \times 10^{14}$ cells or $\sim 29 \text{ g C}$ (Main Text Table 2). This is likely to be a conservative estimate, as cells in the background fluids are larger on average based on microscopic evidence ($\sim 2.5 \mu\text{m}^3$). Turnover time of biomass was then calculated from the CGE-derived productivity estimate and the biomass standing stock by assuming steady state (i.e. primary productivity is equal to losses by export, remineralization, lysis, etc). The upper and lower limits for turnover time (17-41 hours) reflect the uncertainty in primary productivity estimates derived from CGE, and is consistent with doubling times of cultivated chemolithoautotrophic *Campylobacteria* ranging

from ~1 hour to 16 hours (5, 6)

We do recognize that biomass standing stock and turnover will be sensitive to differences in per-cell biomass, metabolic rates of *in situ* populations, and deviations from steady state.

While per-cell biomass for natural communities can be measured as described above, it is much more difficult to measure cell-specific metabolic rates *in situ* for two main reasons. Firstly, the subseafloor system cannot be directly accessed by current sampling techniques. Secondly, it is very difficult to measure bulk metabolic rates in a system characterized by constant fluid flow since tracers of metabolic activity (e.g. $\text{H}^{13}\text{CO}_3^-$) will be rapidly dispersed. Nonetheless, if per-cell metabolic rates became available in the future, they would allow a more confident estimate of biomass turnover time using the conceptual framework outlined above.

Comparisons with estimates from previous studies. In order to compare our data with the previous estimates of sub-seafloor productivity reported by McCollom and Shock (2), we converted their estimates of biomass wet weight to cell carbon by assuming that dry weight is 1/5 of wet weight and composed of 50% carbon.

Comparison with productivity of microbe-animal symbiotic associations above seafloor.

The other major source of fixed carbon at deep-sea hydrothermal vents is from microbe-animal symbiotic associations. We used previously reported estimates of areal biomass density at low-temperature vents (7) combined with biomass-normalized ΣCO_2 uptake rates (8) to estimate an areal productivity between 1.25×10^3 and 1.13×10^4 $\text{g C} \cdot \text{m}^2 \cdot \text{y}^{-1}$ for animal-microbe chemosynthetic symbioses, using values for the giant tubeworm *Riftia pachyptila*, the dominant megafaunal species on the East Pacific Rise and the most productive symbiosis described to date

(8). While it is difficult to directly compare areal and volumetric primary productivity, sub-seafloor productivity at *Crab Spa* (Main Text Table 2) would be equivalent to $\sim 0.5 - 12 \text{ m}^2$ of animal-microbe symbiotic communities. Given that the animal communities clustered around low-temperature vents such as *Crab Spa* occupy a similar area ($\sim 1 \text{ m}^2$), sub-seafloor and symbiotic primary productivity are likely of a similar magnitude.

Extrapolations to the vent field and global scale. In order to extrapolate our data to the vent field and a global scale, we combined our volumetric primary productivity and standing stock estimates with published estimates of total fluid fluxes through low-temperature vent systems (9). For productivity, this was carried out for both high temperature fluid flux estimates (9) by assuming that all of the high-temperature fluid flow flows through ecosystems with an identical mixing ratio to *Crab Spa* (i.e. 7% hydrothermal fluid), following the approach described in (2). We also carried out a similar calculation using the total estimated global 5°C fluid flux (9) assuming that volumetric productivity was the same as *Crab Spa* for these 5°C fluids. Global standing stock was calculated only from the 5°C fluid flow estimates as in (10).

Additional detail about the comparisons between our data and other studies as discussed in the main text of the paper. Our estimates of volumetric primary productivity can be directly compared to McCollom and Shock (1997) who derived theoretical constraints on sub-seafloor productivity by converting available free energy into ATP yields and subsequently microbial biomass (2). Their often-cited estimate of 38 mg C per L end-member hydrothermal fluid is > 10 times higher than 1.4 – 3.5 mg C per L of end-member hydrothermal fluid reported here despite a similar end-member fluid chemical composition (2). However, their calculations were carried

out assuming a final mixture of only ~1% vent fluid and 99% seawater. This fluid composition maximizes potential microbial activity per unit end-member fluid because it provides enough oxygen to allow for complete oxidation of reduced sulfur compounds. If we use our CGE values and assume that that oxygen/nitrate was sufficient to allow the complete oxidation of all available reduced sulfur at *Crab Spa*, we arrive at values much closer to McCollom and Shock (~33 - 79 % of their estimate). However, microbial sulfur oxidation is clearly limited by oxygen/nitrate supply at our study site (1), as will be the case for all fluids warmer than ~5°C (2). We therefore suggest that values reported here are likely more reflective of natural systems, and represent a lower bound for sub-seafloor productivity *in situ*.

The amount of microbial biomass in the hydrothermal vent sub-seafloor biosphere is even more poorly constrained than *in situ* productivity; only one theoretical estimate has been published by Nakamura and Takai who combined fluid flux, free energy calculations and microbial maintenance energy to estimate sub-seafloor standing stock (10). Here, we provide an independent estimate of sub-seafloor biomass standing stock by assuming that cell-specific metabolic rates reported previously (1) are maximum values for microbial communities found *in situ*. Combining the aforementioned chemical depletions of oxygen/nitrate at Crab Spa (1) with fluid flux measurements (11) we determined the total amount of these chemicals consumed by sub-seafloor microbial metabolism and a minimum number of cells necessary to account for this consumption. Converting cell numbers to biomass with a conservative value of ~300 fg C cell⁻¹, we estimate that ~ 1 x 10¹⁴ cells or ~ 29 g C are present in the sub-seafloor at our study site.

Global sub-seafloor standing stock can be calculated using the same fluid flux values used by Nakamura and Takai (10), and yields a value more than three orders of magnitude lower (Main Text Table 2) (10). This large difference is likely due to Nakamura and Takai's

assumption that cells in the sub-seafloor are non-growing and require only maintenance energy to survive (10), which is about three orders of magnitude lower than the amount of chemical energy needed to maintain growing cells (10). Our work shows that sub-seafloor microbes are active and grow rapidly during incubations, implying that cells are unlikely to be in a "maintenance mode" *in situ*. Therefore, while Nakamura and Takai's estimate provides a maximum constraint on sub-seafloor microbial biomass, ours is likely to be closer to the true value.

We can also generalize our data to constrain biomass export from the sub-seafloor into the food-limited deep sea. This was accomplished by multiplying fluid flux at our study site (11) and the relatively well-studied surrounding vent field (12) by volumetric primary productivity values (Main Text Table 2). Compared to the small amounts of photosynthetic primary productivity reaching this depth ($0.4 - 4 \text{ g C m}^{-2} \text{ y}^{-1}$ (7)), sub-seafloor chemosynthetic productivity in the vent field area ($10^3 - 10^4 \text{ m}^2$ (12)) is at least 95 and at most 23,000 times greater than photosynthetic carbon flux to the same area (13) (Main Text Table 2). While it is still unknown what proportion of newly-produced biomass is exported from the sub-seafloor to the water column, even a small fraction would be significant given that photosynthetic carbon reaching these depths will be mostly composed of recalcitrant organic matter. Therefore, sub-seafloor chemosynthesis can vastly increase the availability of labile carbon for heterotrophic consumers on a local scale.

Global biomass export from the sub-seafloor can be similarly constrained by considering estimates of both high- and low-temperature fluid flux (9). As discussed above, lower temperature fluids have a higher ratio of oxygen to reduced sulfur and can consequently support higher amounts of biomass. We therefore used low-temperature (5°C) and high-temperature

(350°C) fluid flux values to calculate a lower and upper bound on global sub-seafloor productivity, respectively (Main Text Table 2). These estimates suggest that sub-seafloor chemosynthetic productivity at deep-sea hot springs represents at most 0.43 % of photosynthetic primary productivity reaching depths > 2000 m (13).

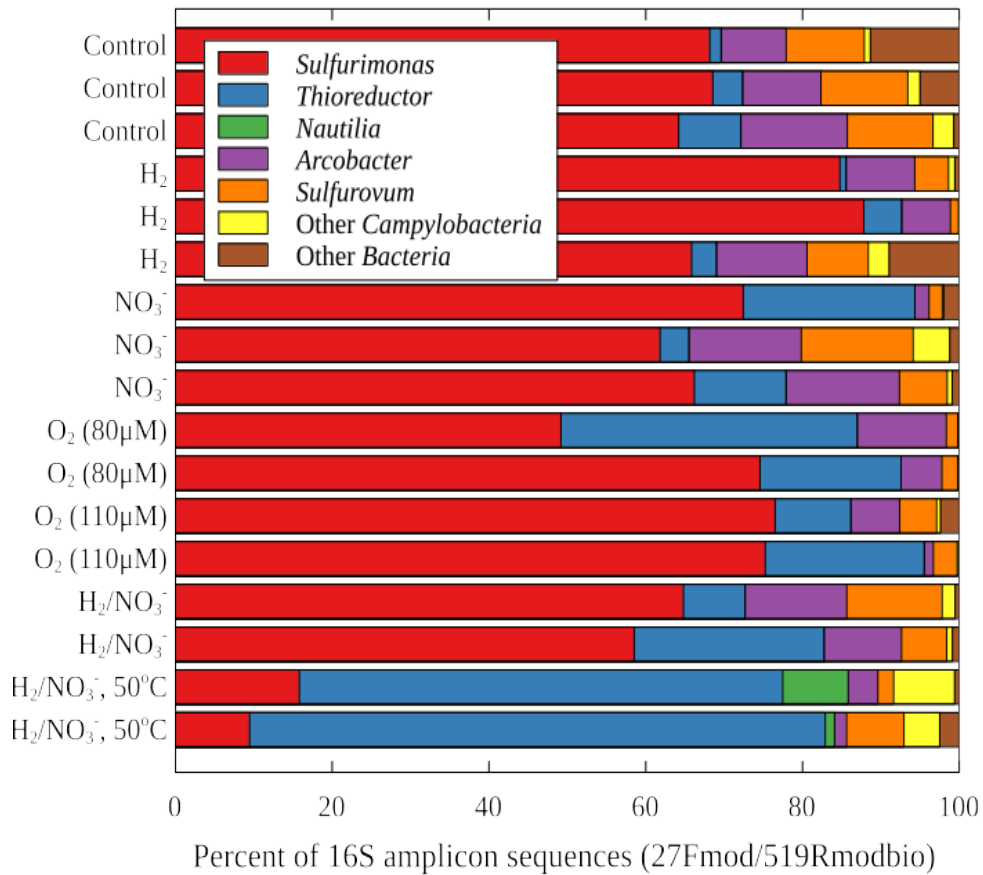


Fig S1: 16S amplicon-based microbial community composition at the end of incubations. All bars represent summed sequences that could be assigned to specific genera of *Campylobacteria* except for “Other *Campylobacteria*” (unclassified *Campylobacteria*) and “Other *Bacteria*” (all other groups).

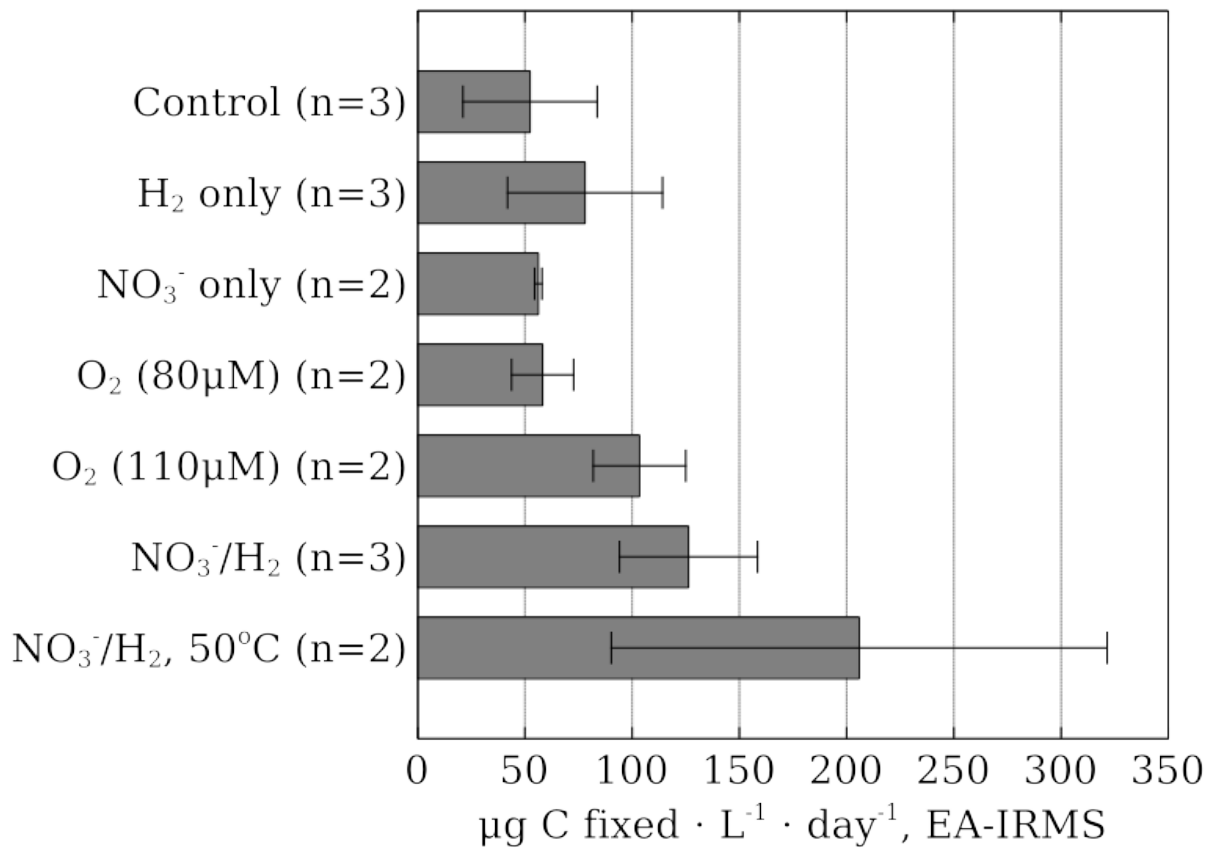


Fig S2: Absolute carbon fixation rates across different treatment conditions. Values were derived by combustion of unfixed bulk microbial biomass and subsequent elemental analysis/isotope-ratio mass spectrometry (EA-IRMS). Errors are standard deviations (n=3), or ranges (n=2).

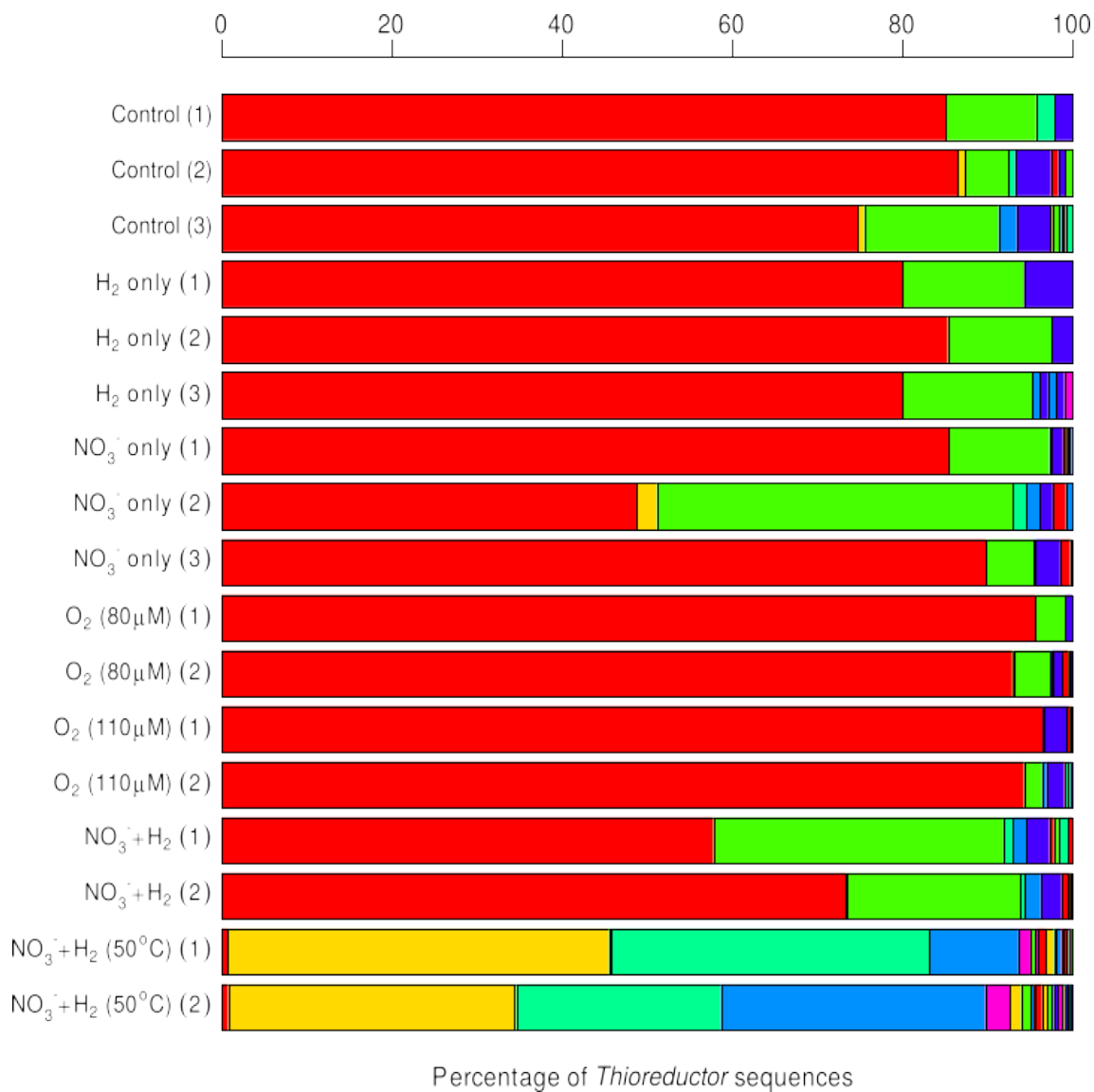


Figure S3: *Thioreductor* 97% OTU composition across different treatment conditions. Each bar represents the abundance of a particular 97% OTU assigned to the genus *Thioreductor*.

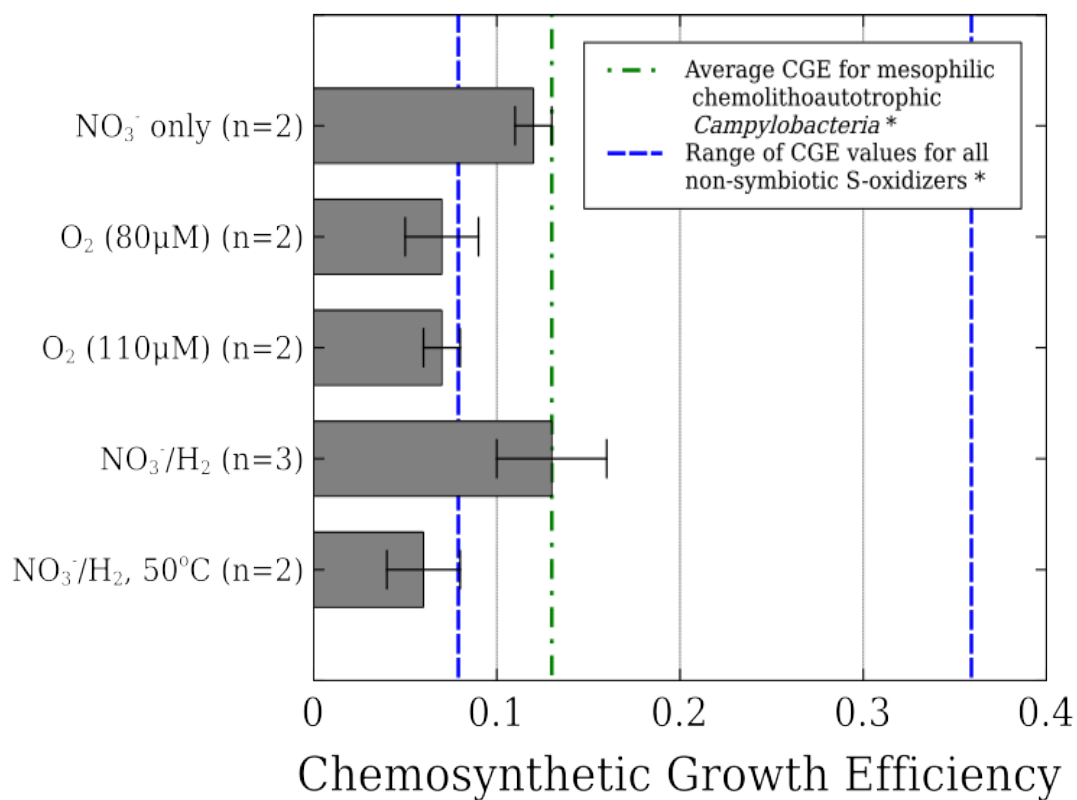


Fig S4: Fraction of electrons from electron donors used for carbon fixation (chemosynthetic growth efficiency). Values were determined from concomitant measurements of absolute carbon fixed and nitrate/oxygen consumed in high-pressure incubations under deep sea conditions. Errors are standard deviations (n=3), or ranges (n=2). * Values from (14).

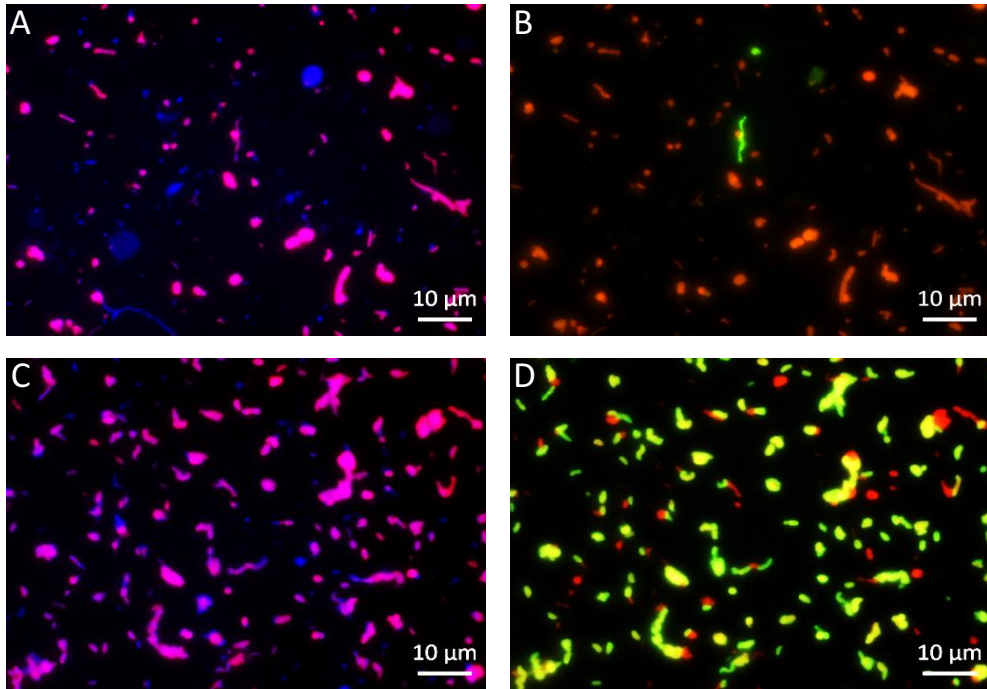


Fig. S5: Epifluorescence micrographs of cells hybridized with the HRP-labelled oligonucleotide probe combination EPSI549/914 (Specific to *Campylobacteria*) and the newly designed probe NAUT921 (Specific to the sub-group *Nautiliales* within the *Campylobacteria*). Sequential deposition of Alexa594 and Alexa488 tyramides for each different probe respectively was conducted on (A and B): untreated *Crab Spa* vent fluid samples preserved immediately after collection, and (C and D): incubations of *Crab Spa* vent fluid with amendments of NO_3^- (100 μM), H_2 (~150 μM) and 10% $\text{H}^{13}\text{CO}_3^-$ at 50°C and ambient deep-sea pressure. Images A/C show the overlay of hybridized *Campylobacteria* cells (red) and DAPI stained cells (blue). Images B/D show dual-hybridized cells with both EPSI and NAUT probes (light green/yellow) and in red cells that hybridized with the EPSI549/914 probe exclusively. Scale bar = 10 μm .

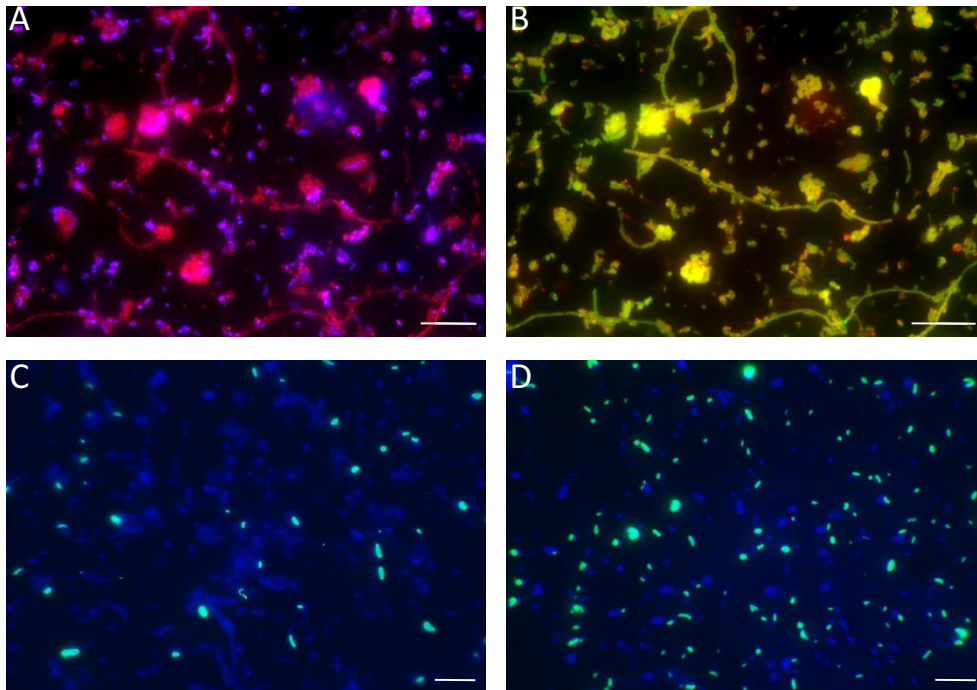


Fig. S6: Epifluorescence micrographs of cells hybridized with the HRP-labelled oligonucleotide probe combination EPSI549/914 (Specific to *Campylobacteria*) and the newly designed probe SFMN287 (Specific to the genus *Sulfurimonas* within the *Campylobacteria*). Figures A & B show the result of testing probes for specificity to the *Campylobacteria* on vent fluid sample amended with O₂ (110μM) and incubated at atmospheric pressure. Sequential deposition of Alexa594 and Alexa488 tyramides for each different probe respectively was conducted to produce images shown in A and B. Image A shows the overlay of hybridized *Campylobacteria* cells (red) and DAPI stained cells (blue). Image B shows dual-hybridized cells with both EPSI and SFMN probes (light green/yellow) and cells that hybridized with the EPSI549/914 probe exclusively (red). Images C & D show the abundance of SFMN287-hybridized cells as an overlay of hybridized *Sulfurimonas* cells (green) and DAPI stained cells (blue). Panel C shows untreated fluids collected from the *Crab Spa* vent and immediately preserved, while panel D shows fluids incubated at 24°C and deep-sea pressure with amendments of O₂ (110μM; D). Scale bar = 10 μm in all images.

Table S1.

Proportion of cells affiliated to different taxonomic groups under different incubation conditions as determined by hybridization with specific oligonucleotide probes using catalyzed reporter deposition fluorescence in-situ hybridization (CARD-FISH). Multiple values correspond to independent replicates.

Condition	Incubation Temperature	<i>Bacteria</i> ¹	<i>Campylobacteria</i> ¹	<i>Sulfurimonas</i> ²	<i>Nautiliales</i> ³	<i>Gammaproteobacteria</i> ⁴
	(°C)	(% DAPI)	(% DAPI)	(% DAPI)	(% DAPI)	(% DAPI)
Background (no incubation)	NA	92.6, 94.6	84.6, 76.2	34.4, 30.3	6.8, 8.4	4.3, 23.8
Control	24	90.1, 93.4, 98.4	66.8, 101.1, 95.7	35.9, 68.1, 62.2	3.5, 4.9, 5.8	30.2, 13.5, 5.2
H₂ addition	24	90.9, 90.1, 101.6	98.4, 69.8, 77.3	76.7, 74.8, 65.8	2.1, 3.0, 2.8	2.0, 7.2, 12.8
NO₃⁻ addition	24	101.3, 99.1, 101.8	100.5, 97.9, 95.1	72.5, 69.7, 68.9	28.8, 6.1, 5.3	16.9, 3.6, 5.8
O₂ addition (80μM)	24	94.2, 98.1	99.4, 99.1	84.1, 84.4	5.0, 20.0	6.2, 2.5
O₂ addition (110μM)	24	96.1, 96.8	102.8, 97.3	74.0	16.7, 16.7	7.0, 1.7
H₂/NO₃⁻ addition	24	98.4, 99.5, 99.0	98.1, 97.3, 105.2	85.2, 85.9, 75.8	11.1, 19.0, 17.5	2.2, 1.8, 8.6
H₂/NO₃⁻ addition	50	94.4, 97.3	93.6, 100.8	19.7, 14.8	83.9, 84.5	11.0, 11.3

1 – EUBI-III; EPSI549/914, see (14) for details; 2 - SFMN287 (this study); 3 - NAUT921 (this study); 4 - GAM42A (15)

Table S2.

Probe sequences used in this study and predicted coverage based on testprobe (<http://www.arb-silva.de/search/testprobe/>). Sequences presented in 5'=>3' direction.

	NAUT921	SFMN287
Probe sequence	TTGTTCCGGGTCCCCGTCT	ATCCTCTCAAACCCGCTA
Competitor sequence(s)	TTGTGCGGGTCCCCGTCT	ATCCTCTCAAACCCCTA
		ATCCTCTCAGACCCGCTA
		ATCCTCTCAAACCAGCTA
		GTCCTCTCAAACCCGCTA
Helper sequence(s)	ATTCCTTTGAGTTTTA	CAGTACCAGTGTGGCGGATC
	CCACATGCTCCACCGC	
Positive control	<i>Caminiabacter mediatlanticus</i>	<i>Sulfurimonas autotrophica</i>
1-mismatch	<i>Sulfurimonas denitrificans</i>	<i>Thiomicrospira halophila</i>
	<i>Sulfurovum lithotrophicum</i>	
	<i>Pseudomonas putida</i>	
Other controls	Natural vent fluid samples (double-hybridization with EPSI549/914)	Natural vent fluid samples (double-hybridization with EPSI549/914)
Formamide (%)	30-40	35
Predicted coverage and notes	High coverage for <i>Nautiliales</i> * (as of May 7 th , 2018, covers 97.2% of all <i>Nautiliales</i> sequences in the SILVA 132 database). Competitor is for <i>Campylobacteriales</i> which are 1-mismatch from probe.	High coverage for taxonomically-diverse <i>Sulfurimonas</i> sequences based on environmental sequence data (as of May 7 th , 2018, covers 75.9% of all <i>Sulfurimonas</i> sequences in the SILVA 132 database).

**Nautiliales* as defined by the unofficial taxonomy presented on the SILVA testprobe website (<https://www.arb-silva.de/search/testprobe/>). By the current definition (SILVA 132, May 2018), *Nautiliales* includes the validly described genera *Caminiabacter*, *Lebetimonas*, *Nautilia*, and *Thioreductor*.

Dataset S1 – See separate excel spreadsheet.

References:

1. McNichol J, et al. (2016) Assessing microbial processes in deep-sea hydrothermal systems by incubation at in situ temperature and pressure. *Deep Sea Res Part I Oceanogr Res Pap* 115:221–232.
2. McCollom TM, Shock EL (1997) Geochemical constraints on chemolithoautotrophic

- metabolism by microorganisms in seafloor hydrothermal systems. *Geochim Cosmochim Acta* 61(20):4375–4391.
3. Lee S, Fuhrman JA (1987) Relationships between biovolume and biomass of naturally derived marine bacterioplankton. *Appl Environ Microbiol* 53(6):1298–1303.
 4. Musat N, et al. (2014) The effect of FISH and CARD-FISH on the isotopic composition of ^{13}C - and ^{15}N -labeled *Pseudomonas putida* cells measured by nanoSIMS. *Syst Appl Microbiol* 37(4):267–276.
 5. Mino S, Kudo H, Arai T, Sawabe T, Takai K, Nakagawa S (2014) *Sulfurovum aggregans* sp. nov. a hydrogen-oxidizing, thiosulfate-reducing chemolithoautotroph within the *Epsilonproteobacteria* isolated from a deep-sea hydrothermal vent chimney, and an emended description of the genus *Sulfurovum*. *Int J Syst Evol Microbiol* 64:3195–3201.
 6. Labrenz M, Grote J, Mammitzsch, Boschker HTS, Laue M, Jost G, Glaubitz S, Jürgens, K (2013) *Sulfurimonas gotlandica* sp. nov., a chemoautotrophic and psychrotolerant epsilonproteobacterium isolated from a pelagic redoxcline, and an emended description of the genus *Sulfurimonas*. *Int J Syst Evol Microbiol* 63:4141–4148.
 7. Fustec A, Desbruyeres D, Laubier L (1988) Estimation de la biomasse des peuplements associés aux sources hydrothermales profondes de la dorsale du Pacifique oriental à 13 degree N. *Oceanol Acta Spec Issue*. Available at: <http://archimer.ifremer.fr/doc/00267/37823/>.
 8. Girguis PR, Childress JJ (2006) Metabolite uptake, stoichiometry and chemoautotrophic function of the hydrothermal vent tubeworm *Riftia pachyptila*: responses to environmental variations in substrate concentrations and temperature. *J Exp Biol* 209(18):3516–3528.
 9. Elderfield H, Schultz A (1996) Mid-ocean ridge hydrothermal fluxes and the chemical composition of the ocean. *Annu Rev Earth Planet Sci* 24(1):191–224.
 10. Nakamura K, Takai K (2015) Geochemical constraints on potential biomass sustained by subseafloor water–rock interactions. *Subseafloor Biosphere Linked to Hydrothermal Systems* (Springer), pp 11–30.
 11. Germanovich LN, Hurt RS, Smith JE, Genc G, Lowell RP (2015) Measuring fluid flow and heat output in seafloor hydrothermal environments. *J Geophys Res Solid Earth* 120(12):8031–8055.
 12. Lowell R, Farough A, Germanovich L, Hebert L, Horne R (2012) A vent-field-scale model of the east Pacific rise 9°50'N magma-hydrothermal system. *Oceanography* 25(1):158–167.
 13. Lampitt RS, Antia AN (1997) Particle flux in deep seas: regional characteristics and temporal variability. *Deep Sea Res Part Oceanogr Res Pap* 44(8):1377–1403.

14. Klatt JM, Polerecky L (2015) Assessment of the stoichiometry and efficiency of CO₂ fixation coupled to reduced sulfur oxidation. *Aquat Microbiol* 6:484.
15. Manz W, Amann R, Ludwig W, Wagner M, Schleifer K-H (1992) Phylogenetic oligodeoxynucleotide probes for the major subclasses of *Proteobacteria*: problems and solutions. *Syst Appl Microbiol* 15(4):593–600.